Raman Difference Studies of GDP and GTP Binding to c-Harvey ras[†]

J. H. Wang,[‡] D. G. Xiao,[‡] H. Deng,[‡] Martin R. Webb,[§] and Robert Callender*[,||,⊥]

Department of Physics, The City College of the City University of New York, New York, New York 10031, National Institute for Medical Research, Mill Hill, London, NW7 1AA, U.K., and Department of Biochemistry, Albert Einstein College of Medicine, Bronx, New York 10461

Received March 2, 1998; Revised Manuscript Received June 5, 1998

ABSTRACT: The vibrational spectra of phosphate modes for GDP and GTP bound to the c-Harvey $p21^{ras}$ protein have been determined using ^{18}O isotope edited Raman difference spectroscopy. A number of the phosphate stretch frequencies are changed upon GDP/GTP binding to ras, and the results are analyzed by ab initio calculations and through the use of empirical relationships that relate bond orders and bond lengths to vibrational frequencies. Bound GDP is found to be strongly stabilized by its interactions, mostly electrostatic, with the active site Mg^{2+}. Bound GTP also interacts with the active site Mg^{2+} via its β-phosphate group, as expected on the basis of crystallographic studies of bound GppNp. The angle between the nonbridging P···O bonds of the γ-phosphate of bound GTP increase by about 1−2° compared to its solution value, thus bringing about a geometry that is closer to planar for these bonds as expected for the putative pentacoordinated transition state geometry of the phosphotransfer reaction. Modeling of the interactions at the nucleotide binding site suggests that the water molecule in-line with the P−O bond is positioned to bring about the change in bond angle. Moreover, a weak fifth bond (about 0.03 vu) appears to be formed between it and the γ-phosphorus atom of bound GTP with a concomitant weakening of the O−P bond between the GDP leaving group and the γ-phosphorus atom. Hence, an important role of the active site structure appears to be the strategic positioning of this in-line water. These structural results are consistent with a reaction pathway for GTP hydrolysis in ras of synchronous bond formation between the γ-phosphorus of GTP and the attacking nucleophile and bond breaking between the γ-phosphorus and the GDP leaving group.

Guanine nucleotide binding proteins are involved in a variety of key cellular processes such as signal transduction, cell growth and differentiation, protein synthesis, and protein transport. They share common sequence elements and have a highly homologous structure (*1*−*4*), and their biochemical activities are tightly regulated by the nature of the bound nucleotide. In general, these proteins are in an "active" state when complexed with GTP and in an "inactive" state when complexed with GDP. The longer a guanine nucleotide binding protein remains in its active GTP-bound state, the longer its particular signal is transmitted and amplified. Hence, the rate of GTP hydrolysis is of great importance for the right timing of many processes in a cell and in vivo. The rate is increased through interaction with other proteins, particularly GTPase activating proteins. Thus, there is substantial interest in understanding the mechanism of the GTPase reaction in guanine nucleotide binding proteins.

The interactions between GDP/GTP and guanine nucleotide binding proteins are not fully understood, although there has been much progress from X-ray and other structural analyses (for a review, see ref *1*). It is generally believed that phosphotransfer involving monoester dianionic phosphate in aqueous solution is primarily via a dissociative pathway, with a metaphosphate-like transition state (ref *5*, and references therein). Here, the bond breaking of the original ester P−O bond is almost complete before significant formation of the new P−O bond, and the sum of the bond orders of the broken and new bond is significantly less than one. However, both associative and dissociative transition states have been proposed for phosphotransfer in enzymes (for example, see refs *6*−*15*).

In this paper, we use Raman difference spectroscopy to study ras, a protein which plays a central role in signal transduction pathways controlling cell proliferation. It has been shown that this technique is well-suited for the determination of the vibrational spectra of ligands bound to proteins (*16*). In one approach, the Raman spectra of the protein−ligand and that of the protein complex alone are measured. The difference spectrum contains bands arising from the bound ligand group. This method cannot be used in our study of the ras protein because the enzyme is unstable without a bound nucleotide. We therefore have employed isotope editing procedures. In our previous studies, an isotopic tag was substituted on positions of the guanine ring in order to obtain the ring's spectra and, hence, study the interactions between the guanine ring and the ras protein (*17*, *18*). Here, the bound nucleotide is replaced by an isotopically (^{18}O) substituted nucleotide of the phosphate moieties

[†] This research was supported by grants from the Institute of General Medicine of NIH, U. S. Public Health Service (GM35183).

* Author to whom correspondence should be addressed. Telephone: 718-430-3024. Fax: 718-430-8565. E-mail: call@aecom.yu.edu.

[‡] City College.

[§] National Institute for Medical Research.

[||] Albert Einstein College of Medicine.

[⊥] On leave from The City College of the City University of New York.

S0006-2960(98)00471-1 CCC: $15.00
Published on Web 07/17/1998

of GDP and GTP, and the spectra of the protein−nucleotide and protein−(^{18}O)nucleotide are taken. The difference spectrum formed from these spectra arise from motions of the labeled P−O bonds. Hence, our goal in this study is the bond properties of the phosphate groups of GDP and GTP bound to ras.

Assignment of the Raman bands in the ^{18}O derived difference spectra is made on the basis of comparisons to the parent spectra in aqueous solution previously reported (*19*), considerations of bandwidths and intensities that vary for various normal modes, and the ^{18}O frequency shifts that are evident in the difference spectra. There are a number of changes in the peak positions of many phosphate bands of GDP and GTP upon binding to ras, which have implications for both how these molecules bind and the hydrolysis mechanism. The spectral changes are analyzed by employing known empirical relationships between bond orders/lengths and frequencies as well as vibrational analyses from ab initio calculations. The absolute accuracy of determining bond lengths and bond orders of the nonbridging P⋯O bonds determined from the empirical correlations relating the vibrational stretch frequencies to these quantities (*20*, *21*) is very high compared to protein crystallographic studies, about ±0.04 vu and ±0.004 Å for bond orders and bond lengths, respectively. The accuracy in determining changes in these parameters when a specific molecule is moved from one environment to another is probably about a factor of 5 more accurate. In addition, it is possible to determine the nonbridging O⋯P⋯O bond angles.

MATERIAL AND METHODS

Materials. GDP and GTP were purchased from Sigma or Boerhinger Mannheim. The ^{18}O-substituted GDP and GTP (91−92% enriched in each position) were synthesized as described previously (*19*). Ras·GDP was purified from the *Escherichia coli* strain RRIDM 15 containing the ptac-c-H-ras plasmid (*22*). The expression system was a generous gift from Dr. A. Wittinghofer (Dortmund, Germany). Proteins were >95% pure as judged by SDS−PAGE. All preparations were analyzed for their nucleotide content by RP-HPLC (*23*, *24*). Purified protein was stored at −76 °C in buffer A (50 mM Tris-HCl, pH 7.6, 10 mM $MgCl_2$, 0.5 mM DTE, 1 mM NaN_3, 0.1 mM PMSF) containing 0.1 mM GDP, and was routinely checked for its activity using a radioactive GDP binding assay (*25*).

Ras complexed with (^{18}O)GDP(GTP) was prepared in two stages: first, protein was complexed with GppCp in the presence of alkaline phosphatase (agarose or acrylic beads linked; Sigma Chemical Co., St. Louis, MO) (*23*). When all of the GDP was converted (after ∼1 h) as assessed by RP-HPLC, the phosphatase was removed by filtration. Ras·GppCp was isolated by passing the solution through a PD-10G25 column (Pharmacia-LKB, Piscataway, NJ) to remove excess GppCp. The protein was then was incubated for 45 min at 25 °C with 5-fold molar excess of (^{18}O)GDP(GTP) in buffer I (200 mM Tris-HCl; 200 mM $(NH_4)_2SO_4$; 0.55 mM DTT; 0.5 mM NaN_3; 0.6 mM EDTA; pH 7.5). Just before the Raman experiment, the sample was washed three times with buffer T (20 mM Tris-HCl; 10 mM $MgCl_2$; 0.5 mM NaN_3; pH 7.5) using a Centricon 10 (Amicon) at 8000 rpm.

Raman Spectroscopy. Raman spectra were measured by an optical multichannel analyzer (OMA) system consisting of a Triplemate spectrometer (Spex Industries, Metuchen, NJ) and a charge coupled device (CCD, Model LN/CCD-1152UV liquid-nitrogen-cooled and a model ST-135 detector; Princeton Instruments). The detector was interfaced to a Macintosh computer (Apple, Cupertino, CA). Spectral lines were calibrated against known assignments of toluene. All Raman spectra shown in the following figures were obtained by using 568.2-nm lines of a krypton ion laser (Coherent Radiation Inc., Palo Alto, CA) at about 150 mW. Isotope editing of the Raman spectra was performed in the following manner. Separate spectra for enzyme·nucleotide and isotopically substituted enzyme·nucleotide complexes in solution, approximate concentration 5 mM, were measured using a special split cell (the volume of each side being about 30 μL) and a sample holder with a linear translator as previously described (*18*, *26*, *27*). The spectrum of one side of the split cuvette is taken, the split cell is translated, and the spectrum of the other side is taken. This sequence is repeated until sufficient signal-to-noise is obtained. A difference spectrum is generated by numerically subtracting the sum of the spectra obtained from each side. In general, the two summed spectra do not subtract to zero, as judged by the subtraction of well-known protein marker bands. These protein marker bands are determined from their bandwidths (generally much broader than those of spectra from bound substrates) and their characteristic positions. Hence, one summed spectrum is scaled by a small numerical factor, generally between 1.05 and 0.95, which is adjusted until the protein bands are nulled. As an example, the summed spectra and the difference spectra generated by numerical factors somewhat larger to somewhat smaller than that used to generate the difference spectrum in Figure 2b below are shown in the Appendix. In addition to the primary spectra, a control difference spectrum is generated whereby the protein binary complex sample is used to generate both the sample as well as the reference spectra. Our Raman difference spectrometer is able to obtain difference spectra smaller than 0.1% of the protein background bands (accuracy of better than 0.2% is shown here). All marked bands have been observed in at least four different runs. The same control procedures were performed on all of the difference spectra results herein. Resolution of the spectrometer is 8 cm^{-1} for the present results. A spectral calibration is done for each measurement using the known Raman lines of toluene, and absolute band positions are accurate to within ±2 cm^{-1}. None of the spectra presented here have been smoothed.

RESULTS

We have determined the Raman spectra of GDP and GTP bound to the ras protein from Raman difference spectroscopy

[1] Abbreviations: vu, valence unit (a measure of bond order based on atomic valence); α-O_2 refers to the nonbridging oxygens of the α-group of GDP or GTP and similarly for β-O_3 (in GDP) or β-O_2 (in GTP) and γ-O_3 (in GTP); αβ-O is the bridging oxygen between the α- and β-phosphates of GDP or GTP and βγ-O is the bridging oxygen between the β- and γ-phosphates of GTP; (β-$^{18}O_3$)GDP, the three nonbridging oxygen atoms of the β-phosphate group are replaced by ^{18}O; (α,β-^{18}O;β-$^{18}O_3$)GDP, the four oxygen atoms of the β-phosphate group are replaced by ^{18}O; (β-$^{18}O_2$;βγ-^{18}O)GTP, the two nonbridging oxygen atoms of the β-phosphate group as well as the bridging oxygen atom of $P_β$-O-$P_γ$ are replaced by ^{18}O; (γ-$^{18}O_3$)GTP, the three nonbridging oxygen atoms of the γ-phosphate group are replace by ^{18}O.

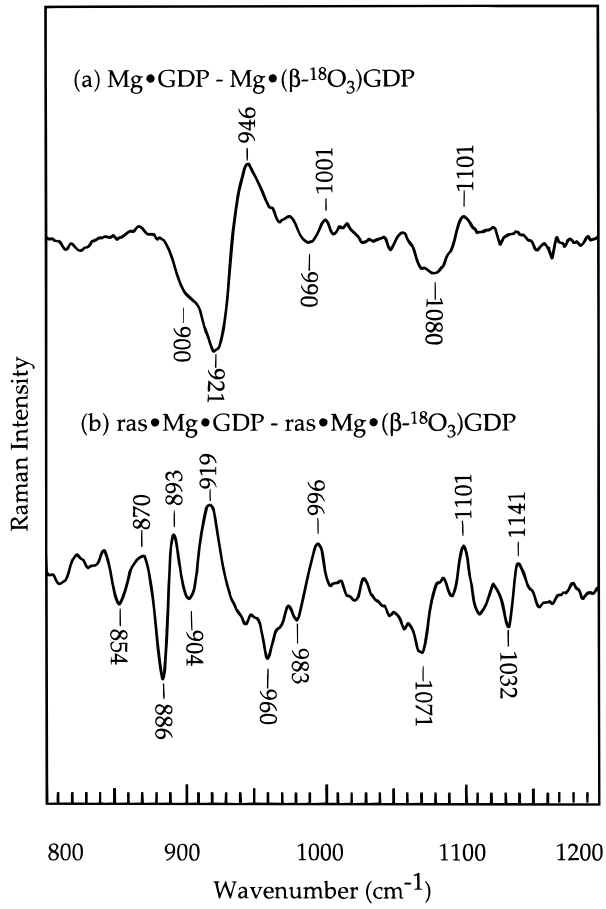

FIGURE 1: Raman difference spectra of Mg·GDP minus Mg·(β-$^{18}O_3$)GDP in (a) aqueous solution and (b) ras, both at pH 7.5. The temperature of the sample was maintained at 4 °C during the Raman measurements.

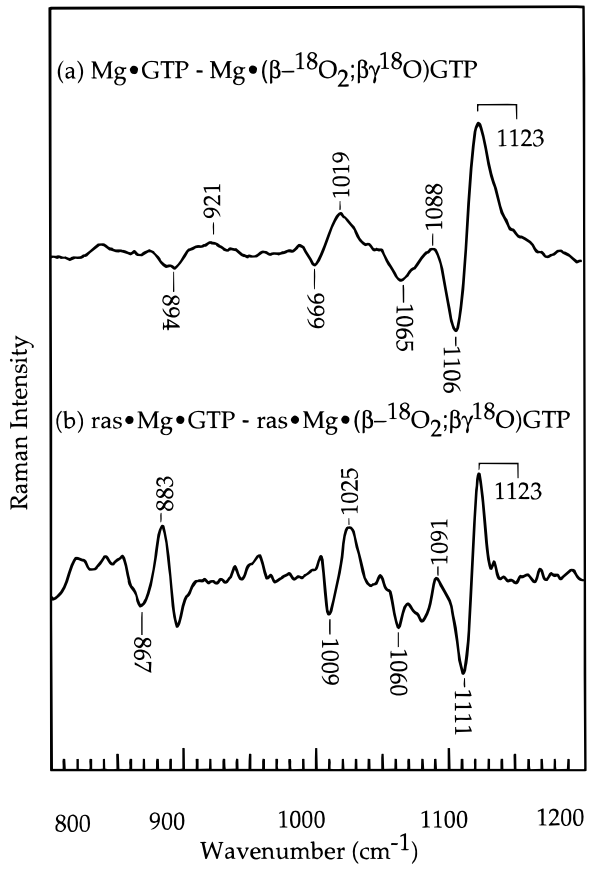

FIGURE 2: Raman difference spectra of Mg·GTP minus Mg·(β-$^{18}O_2$;$\beta\gamma$-^{18}O)GTP in (a) aqueous solution and (b) ras, both at pH 7.5. The temperature of the sample was maintained at 4 °C during the Raman measurements.

(*16*) using isotope editing techniques (*17, 18*). Since isotope labeling induces spectral shifts of the vibrational modes associated with motions of the labeled atom, all Raman bands, including those of the apoprotein and those of the bound nucleotide that do not involve the isotopic tag, cancel out in the difference spectrum. In the results reported here, difference spectra are obtained by ^{18}O labeling of the nucleotide P⋯O bonds and incorporating these nucleotides into the binding site. The ^{18}O-substitution typically shifts P⋯O stretch bands downward 20−40 cm^{-1}. The ^{16}O-associated bands show up as positive features while the ^{18}O-substituted spectra show up as negative bands in the difference spectrum, yielding typically a positive/negative couple. There are many positive/negative features in the difference spectra presented below, which would ordinarily make assignments quite difficult. However, accurate band assignments of the solution difference spectra can be made largely on the basis of the previously reported parent spectra (*19*) since the individual bands are observed as are their shifts upon ^{18}O-substitution. Then a comparison is made between these difference spectra and their corresponding protein difference spectra to assign the protein difference spectra. A similar pattern was typically observed except that the spectral bandwidths are almost always relatively smaller for the protein spectra and, additionally, band shifts of the positive/negative couple may be observed. Bandwidth narrowing for protein-bound ligands is well understood and comes about because proteins typically limit conformational flexibility of small bound molecules, which reduces heterogeneous line broadening. Generally, more bands are observed in the protein difference spectra than in the solution difference spectra because what were overlapping bands now become resolved. Many of these newly observed bands cannot be assigned easily.

Raman Spectra of GDP. Figure 1a shows the Raman difference spectrum of GDP and (β-$^{18}O_3$)GDP with 1:1 molar $MgCl_2$ in aqueous solution at pH 7.5. At pH 7.5, the diphosphate moiety of GDP is composed of a $>PO_2^-$ group and a $-PO_3^{2-}$ terminal group. The PO_3^{2-} group has approximate C_{3v} symmetry yielding a symmetric P⋯O stretch mode, υ_s(β-PO_3^{2-}), and a doubly degenerate antisymmetric P⋯O stretch mode, υ_a(β-PO_3^{2-}). The $>PO_2^-$ group has approximate C_{2v} symmetry which leads to a symmetric stretch mode, υ_s(α-PO_2^-), and an antisymmetric mode υ_a-(α-PO_2^-). In addition, there are P−O single bond stretch modes of the P−O−P linkage.

The positive/negative features at 946/900, 1001/990, and 1101/1080 cm^{-1} (the high frequency denoting the ^{16}O peak position and the low frequency denoting the ^{18}O position) arise from the symmetric P⋯O stretch mode, υ_s(β-PO_3^{2-}) of the β-PO_3^{2-} group, a mode involving significant P−O stretch mode υ(P−O) of the P_α−O−P_β linkage, and the symmetric stretch mode, υ_s(α-PO_2^-), of the α-PO_2^- group, respectively (*19*). The assignment of the 1001/990 cm^{-1} couple is based upon the Raman spectrum of GDP (*19*) as well as the Raman difference spectrum of GDP and ($\alpha\beta$-^{18}O;β-$^{18}O_3$)GDP since a strong derivative feature appears at 1002/982 cm^{-1}

Table 1: The Frequencies (in cm^{-1}) of the Phosphate Modes of Mg·GTP in 1:1 Complex in Aqueous Solution and Their Shifts for Mg·GDP/GTP Bound to ras

	mode	aqueous solution[a]	ras($\Delta\upsilon$)
GDP	$\upsilon_{st}(P_\alpha\text{-}O\text{-}P_\beta)$[b]	921	−28
	$\upsilon_s(\beta\text{-}PO_3^{2-})$	942 (946)	−27
	$\upsilon_{st}(P_\alpha\text{-}O\text{-}P_\beta)$[b]	1001	0
	$\upsilon_s(\alpha\text{-}PO_2^-)$	1094 (1101)	0
	$\upsilon_a(\beta\text{-}PO_3^{2-})$	1123	−23[c]
	$\upsilon_a(\alpha\text{-}PO_2^-)$	1215	+21[c]
GTP	$\upsilon_{st}(P_\beta\text{-}O\text{-}P_\gamma)$[b]	921	−38
	$\upsilon_s(\gamma\text{-}PO_3^{2-})$	926	−10
	$\upsilon_{st}(P_\beta\text{-}O\text{-}P_\gamma)$[b]	1019	+6
	$\upsilon_a(\gamma\text{-}PO_3^{2-})$	1128	+12[d]
	$\upsilon_s(\text{in-}PO_2^-)$	1122	0
	$\upsilon_s(\text{out-}PO_2^-)$	1088	+3
	$\upsilon_a(\beta\text{-}PO_2^-)$	1247	−32[c]

[a] The number in parentheses is the peak position observed in the solution difference spectra presented herein. This value is sometimes different than the position in the solution spectra (*19*) due to some intensity cancellation in the difference spectrum when the labeled and nonlabeled bands are separated from each other by an amount smaller than their bandwidths. [b] The modes indicated by $\upsilon_{st}(P_\alpha\text{-}O\text{-}P_\beta)$ contain significant stretch motions of the $P_\alpha\text{-}O\text{-}P_\beta$ linkage as indicated by their shifts in frequency upon ^{18}O substitution of the $P_\alpha\text{-}O\text{-}P_\beta$ oxygen. Similarly for modes indicated by $\upsilon_{st}(P_\beta\text{-}O\text{-}P_\gamma)$. [c] From refs *28, 29*. [d] There are two possible bands that could be assigned to $\upsilon_a(\gamma\text{-}PO_3^{2-})$, at 1128 or 1140 cm^{-1} (refs *28, 29*; see text); the 1140 cm^{-1} is favored.

(unpublished data). Another mode that contains significant P−O stretch motion of the $P_\alpha\text{-}O\text{-}P_\beta$ linkage is found at approximately 941 cm^{-1} (*19*), which shifts down in (β-$^{18}O_3$)-GDP to yield the prominent 921 cm^{-1} negative band in the difference spectrum. This assignment is consistent with the Raman difference spectrum of GDP and ($\alpha\beta$-^{18}O;β-$^{18}O_3$)-GDP in which the 921 cm^{-1} negative band shifts down to 895 cm^{-1}, overlapping the negative band at 900 cm^{-1} (unpublished data). For broad bands where the ^{16}O and ^{18}O band profiles overlap somewhat, there is some cancellation of intensity in the difference spectrum, and the peak frequencies observed in the difference spectrum can be shifted from their proper position [apparently shifting up in the ^{16}O part of the derivative looking band and shifting down in the ^{18}O part of the difference couple for bands where ^{18}O substitution induces a downshift (*18*)]. This has affected the apparent position of $\upsilon_s(\beta\text{-}PO_3^{2-})$, which is observed to be at 946 cm^{-1} in the difference spectrum of Figure 1a. Its actual position in the solution data of GDP is at 942 cm^{-1}. Since the ^{18}O-substituted shifts are generally larger than bandwidths, not many of the band positions are so affected, and the band positions reported in the difference spectra typically report on the actual position. The positions and assignments of the bands are summarized in Table 1.

Figure 1b shows the difference spectrum formed between Mg·GDP and Mg·(β-$^{18}O_3$)GDP when bound to wild-type ras. There are three positive/negative couplets at 919/886, 996/983, and 1101/1071 cm^{-1} (Figure 1b), respectively. These are similar to the solution bands observed at 946/900, 1001/990, and 1101/1080 cm^{-1} (Figure 1a) in strength (allowing for the apparent increased strength that would come about for a band with a reduced bandwidth) and ^{18}O shift, and they can be assigned as the corresponding mode found in solution. The peak positions of the protein-bound nucleotides are very unlikely to be shifted from their true positions because of the substantial band narrowing that results for protein-bound ligands. There is an additional feature at 870/854 cm^{-1} which remains unassigned. The shifts of the bands of bound GDP from their respective solution positions are given in Table 1. The most important result is that both the symmetric stretch, $\upsilon_s(\beta\text{-}PO_3^{2-})$, and the antisymmetric stretch, $\upsilon_a(\beta\text{-}PO_3^{2-})$, whose positions have been determined in FTIR studies (refs *28, 29*; see Table 1), undergo substantial frequency shifts when GDP binds to ras as does $\upsilon_a(\alpha\text{-}PO_2^-)$. X-ray crystallographic studies shows that the only interaction between the α-phosphate group of the bound GDP molecule and protein is a hydrogen bond between an oxygen atom on the α-phosphate and the main-chain amide group of residue Ala18 (*30*). In comparison, the β-phosphate group interacts extensively with residues 13−17 of ras as well as the bound Mg^{2+} (*30*). The downward shifts in frequency show that the nonbridging P⋯O bonds of the β-PO_3^{2-} group are strongly polarized and indicate a strong interaction between protein and the β-PO_3^{2-} group. Below, the change in bond order of the nonbridging P⋯O bonds is calculated based on empirical relationships between bond order and vibrational frequencies.

Raman Spectra of GTP. Raman difference experiments were carried out using two ^{18}O derivatives. In (β-$^{18}O_2$;$\beta\gamma$-^{18}O)GTP, the two nonbridging oxygens of the β-PO_2^- moiety were substituted; in (γ-$^{18}O_3$)GTP, the three nonbridging oxygens of the γ-PO_3^{2-} group were substituted. Figure 2 shows the Raman difference spectrum of GTP and (β-$^{18}O_2$;$\beta\gamma$-^{18}O)GTP with 1:1 $MgCl_2$ in aqueous solution (panel a) and the corresponding difference spectrum between the natural abundance and ^{18}O-substituted nucleotides bound to ras (panel b). Figure 3 shows the corresponding difference spectra using (γ-$^{18}O_3$)GTP. All studies were carried out at pH 7.5. At this pH, the triphosphate moiety of GTP in solution is composed of two PO_2^- groups and one γ-PO_3^{2-} group. The γ-PO_3^{2-} group has approximate C_{3v} symmetry which leads to a symmetric P⋯O stretch mode, $\upsilon_s(\gamma\text{-}PO_3^{2-})$, and a doubly degenerate antisymmetric P⋯O stretch mode, $\upsilon_a(\gamma\text{-}PO_3^{2-})$. The symmetric stretch motions of the two PO_2^- groups are often strongly coupled to form an in-phase combination, $\upsilon_s(\text{in-}PO_2^-)$, and an out-of-phase combination, $\upsilon_s(\text{out-}PO_2^-)$, while two antisymmetric modes, $\upsilon_a(\alpha\text{-}PO_2^-)$ and $\upsilon_a(\beta\text{-}PO_2^-)$, are not strongly coupled. The Raman intensity of the in-phase combination, $\upsilon_s(\text{in-}PO_2^-)$, is much higher than that of the other modes.

In the difference spectrum between the two Mg·GTP complexes (Figure 2a), with unsubstituted and (β-$^{18}O_2$;$\beta\gamma$-^{18}O)nucleotide, there are four major positive/negative couplets at 1123/1106, 1088/1065, 1019/999, and 921/894 cm^{-1}, which can be assigned to P⋯O stretch modes related with β-PO_2^- motions. Based on the frequency shifts of ^{18}O substitution, relative Raman intensities, and the positions of the bands (*19*), the strongest and sharpest Raman derivative-like band at 1123/1106 cm^{-1} (Figure 2a) can be assigned to the in-phase combination, $\upsilon_s(\text{in-}PO_2^-)$, of the α,$\beta$-$PO_2^-$ groups. The weak feature at 1088/1065 cm^{-1} (Figure 2a) is due to the out-of-phase combination, $\upsilon_s(\text{out-}PO_2^-)$. The frequency shifts of $\upsilon_s(\text{in-}PO_2^-)$ and $\upsilon_s(\text{out-}PO_2^-)$ (17 and 23 cm^{-1}, respectively) are less than the ^{18}O shift of the P⋯O symmetric stretch modes in monophosphates (40 cm^{-1}, either monoanionic or dianionic) indicating that there is considerable mixing of PO stretch motions of the α- and β-phosphate groups. The much weaker derivative-like band at 921/894

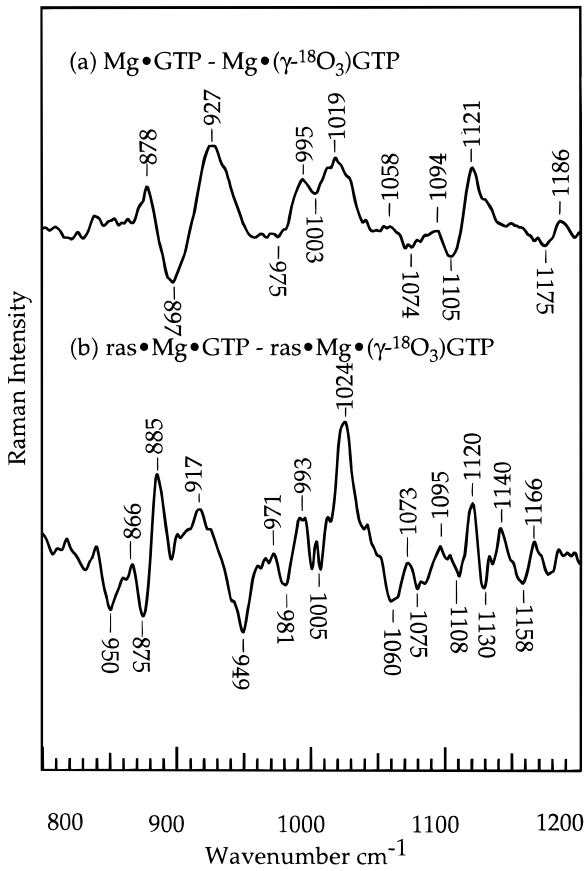

FIGURE 3: Raman difference spectra of Mg·GTP complex minus Mg·(γ-$^{18}O_3$)GTP in (a) aqueous solution and (b) ras, at pH 7.5 and at 4 °C.

cm^{-1} (Figure 2a) most likely contains P−O stretch motions of the P_γ−O−P_β linkage. The other couplet band at 1019/999 cm^{-1} (Figure 2a) is thus assigned to a mode containing P−O stretch motions of the P_α−O−P_β linkage (see Figure 4 in ref *19*).

Figure 2b shows the Raman difference spectrum formed between Mg·GTP and Mg·(β-$^{18}O_2$;$\beta\gamma$-^{18}O)GTP when bound to wild-type ras at pH 7.5. Qualitatively, Figure 2b is very similar to Figure 2a. However, some peak positions are affected by the binding. There are three major couplets at 1123/1111, 1091/1060, 1025/1009, and 883/867 cm^{-1}, respectively, and they are just slightly shifted and maintain their relative intensities compared to the solution bands observed at 1123/1106, 1088/1065, and 1019/999 (Figure 2a). The protein 883/867 cm^{-1} pair (2b), while strongly shifted and substantially narrowed from the corresponding 921/894 cm^{-1} solution pair (2a), appears to be the same mode. Hence, these bands can be assigned to shifted modes as assigned in the solution spectra. This is tabulated in Table 1.

Figure 3a shows the Raman difference spectrum of GTP and (γ-$^{18}O_3$)GTP with 1:1 $MgCl_2$ in aqueous solution at pH 7.5. Upon ^{18}O-substitution at the γ-position, the stretch modes related with γ-PO_3^{2-} group are mostly affected. There are four major positive/negative bands at 1121/1105, 1019/1003, and 927/897 cm^{-1}, respectively, which can be assigned to the P···O/P−O stretch modes. Based on the ^{18}O isotope labeling, relative Raman intensities, and the positions of the bands (*19*), it is clear that the most prominent feature at 927/897 cm^{-1} (Figure 3a) results from the symmetric stretch mode of the γ-PO_3^{2-} group. The 1121/1105-cm^{-1} feature (Figure 3a), which is observed in the Figure 2a, is the in-phase combination υ_s(in-PO_2^-) of α- and β-PO_2^- groups. The much weaker couplet at 1019/1003 cm^{-1} (Figure 3a), which is very similar to 1019/999 cm^{-1} band in Figure 2a, is thus assigned as involving P−O stretch motions of the P_α−O−P_β linkage (*19*).

Figure 3b shows the Raman difference spectrum formed between Mg·GTP and Mg·(γ-$^{18}O_3$)GTP when bound with to ras at pH 7.5. Qualitatively, Figure 3b is very similar to Figure 3a. However, some peak positions are shifted by the binding. The three major positive/negative bands at 1120/1108, 1024/1005, and 917/? cm^{-1} (Figure 3b), respectively, are the corresponding bands in the solution spectrum observed at 1121/1105, 1019/1003, and 927/897 cm^{-1} (Figure 3a). There is also an additional sharp feature at 885 cm^{-1} which is also observed in the ras·Mg·(β-$^{18}O_2$;$\beta\gamma$-^{18}O)-GTP difference spectrum of panel b, Figure 2. Its ^{18}O shift is only 10 cm^{-1} when the γ-PO_3^{2-} group is labeled as opposed to a 16 cm^{-1} shift when the β-PO_2^- group is labeled. This mode is thus fairly extended. The sharp positive 885 cm^{-1} band also obscures the real position of υ_s(γ-PO_3^{2-}) for ras·Mg·(γ-$^{18}O_3$)GTP which is expected to show up as a negative band in the difference spectrum near 890 cm^{-1} (hence, the nomenclature 917/? above). All these results are tabulated in Table 1.

Ab Initio Vibrational Analysis. Ab initio normal-mode analyses were performed to assess how specific interactions contribute to the frequency shifts observed in the binding of GDP and GTP to ras. It is expected that Mg^{2+} interacts strongly with the oxygens and hence alters vibrational frequencies of the polar phosphate bonds. Such interactions will depend on the nucleotide−metal ion distance as well as relative orientation. Hence, the phosphate frequencies are likely affected differently in solution versus in protein as the geometries are different. Moreover, it is of considerable interest to investigate the interaction of the γ-phosphate group with water-175, which is in-line with the P−O bond of ras-bound GTP and is a candidate for the attacking nucleophile. All calculations were performed with the guanosine moiety replaced by a methyl group to simplify them. A sodium ion is used to model the effect of Mg^{2+} interacting with GDP-(GTP) in aqueous solution and in ras. The reduced charge takes partial account of screening of the Mg^{2+} charge by its surrounding medium. In this way, the modeling allows a semiquantitative assessment of the spectral changes that take place when the spatial arrangement of the interacting group with respect to the nucleotide is changed and also provides some idea of the size of the spectral changes that can be expected (*31*−*33*). It must be stressed that the goal of these calculations is not to determine specifically how the nucleotides bind with ras from the vibrational data; that would require modeling of the entire binding site, which is outside our present scope. Rather, we are concerned with assessing which interactions are important, in what way they affect the phosphate stretch frequencies, and how symmetric and antisymmetric modes are affected by a putative interaction. The symmetries of these modes are different, and they shift quite differently depending on the geometry of the interacting atoms.

The calculations presented here were performed at the HF/3-21g* level for the following reasons. Chemical bond

lengths, especially those bonds which contain oxygen, are underestimated by ab initio methods at the Hartree−Fock level compared with observed values (*34*). Moreover, calculated stretch frequencies are in error by about 10−20% due to the neglect of electron correlation forces in the calculations, the limited basis set (particularly severe for phosphorus), and also that the calculations are done in gas phase which does not treat the interactions with solvent. On the other hand, we have systematically determined all the vibrational frequencies of phosphates of varying ionization states in solution (i.e., PO_4^{3-}, HPO_4^{2-}, $H_2PO_4^{1-}$, H_3PO_4, and $CH_3OPO_3^{2-}$) and their ^{18}O-substituted analogues. The gas phase ab initio calculations at the HF/3-21g* level provide an adequate force field over this entire range of ionization states, overestimating double-bond stretches and the ^{18}O shifts by about 15% while underestimating single-bond stretches and their ^{18}O shifts by approximately 6%.[2] Trial runs with higher order basis sets at the Hartree−Fock level did not significantly improve the agreement; post Hartree−Fock calculations were somewhat better but, in view of the limited scope of the calculations herein, do not seem worthwhile given the extensive computer time required. Finally, the HF/3-21g* level basis set does not treat properly the observed coupling between the $-PO_2-$ groups of GTP, probably because of the neglect of electron correlation, and results on these modes are not reported.

It is known that most of the phosphate stretch bands of GDP (or GTP) in solution are affected when the Mg·GDP complex is formed (*19*). In the analyses of the solution complexes, the geometries of the models used to simulate solution conditions were first optimized at the HF/3-21g* level, and the frequency calculations are then performed on the optimized geometries using the same basis set. The result of freely optimizing the geometry indicates that the metal ion binds to both α- and β-phosphates groups (Figure 4, structure **I**), as is known from experimental studies. The P···O bond of the terminal β-PO_3^{2-} group directly interacting with the ion is longer than the other two, slightly breaking the C_{3v} symmetry of the terminal group. The C_{2v} symmetry of α-PO_2^- group is also slightly broken. The approximate symmetry classification of the resultant stretch modes was identified based on calculated Raman intensities and depolarization ratios. Table 2 lists the symmetric mode υ_s(β-PO_3^{2-}) (1050 cm^{-1}) and the average antisymmetric stretch mode, υ_a(β-PO_3^{2-}) (1335 cm^{-1}). For the α-PO_2^- group, the character of the 1234 and 1368 cm^{-1} modes is also quite close to the symmetric and antisymmetric stretch modes for PO_2 with approximate C_{2v} symmetry, respectively. The shifts in frequencies of the phosphate stretch modes induced by the metal ion as obtained by the ab initio procedure adequately reproduce the direction of the shifts experimentally measured, although the magnitude can be overestimated. For example, the relative shifts of the important terminal group (in cm^{-1}) are (calculated, measured): υ_s(β-PO_3^{2-}) (−3, −2); υ_a(β-PO_3^{2-}) (52, 8).

Crystallographic studies of GDP bound to ras indicate that the binding site Mg^{2+} lies in such a way that it interacts

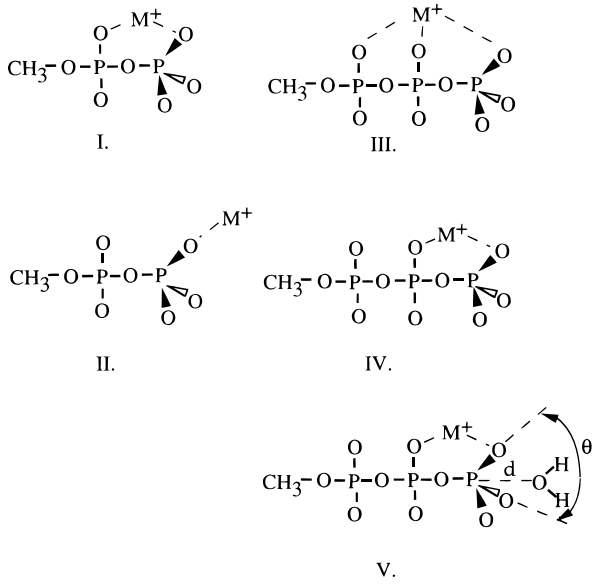

FIGURE 4: The various structures used to model the environment of GDP in solution (**I**) and in ras (**II**) and the environment of GTP in solution (**III**) and in ras (**IV** and **V**).

Table 2: Frequency Shifts[a] of Phosphate Groups of Na·methyldiphosphate (M^+·CH_3DP) and Na·Methyltriphosphate (M^+·CH_3TP) Calculated by ab Initio Methods to the HF/3-21g* Level

	mode	solution model structure **I**	ras·GDP·M^+ structure **II**
M^+·CH_3DP	υ_s(β-PO_3^{2-})	1050	−34
	υ_a(β-PO_3^{2-})	1335	−30
	υ_s(α-PO_2^-)	1234	−1
	υ_a(α-PO_2^-)	1368	+20

		solution model structure **III**	ras·GTP·M^+ structure **IV**	ras·GTP·M^+·H_2O structure **V**
M^+·CH_3TP	υ_c(γ-PO_3^{2-})	1000	+1	−9
	υ_a(γ-PO_3^{2-})	1287	+2	−1

[a] All values are in cm^{-1}.

only with one oxygen atom of the β-phosphate group (cf., Figure 4, structure **II**). To simulate the Mg·GDP (and GTP) bound to ras, the metal ion was placed at various positions relative to the phosphate moiety, restricted so as to be close to the position determined by the X-ray crystallographic studies of ras·GDP. The P···O stretch frequencies of the β-PO_3^{2-} group are quite sensitive to the position of the metal ion since the interaction between the negative charges of $-PO_3^{2-}$ and the positive charge of M^+ changes the O···P···O bond angle significantly. The position of the metal ion that is most consistent with the data is one where the M^+-O-P angle is about 20° from that reported in the X-ray structure; this result is tabulated in Table 2. The calculated υ_s(β-PO_3^{2-}) mode for ras·GDP/M^+ shifts down by 34 cm^{-1} compared to the solution model structure while υ_a(β-PO_3^{2-}) shifts down 30 cm^{-1}. This can be compared to the shifts found experimentally of −27 and −23 cm^{-1}, respectively (Table 1). The shifts found for the α-PO_2^- phosphate stretches are also in very satisfactory agreement with the experimental shifts (compare Tables 1 and 2). Therefore, the present experimental results, and the simulations, are in reasonable agreement with previous conclusions that Mg^{2+} binds to both

[2] More specifically, the double bonds and their frequency shifts are overestimated by 10, 15, 19, 20, and 15% for PO_4^{3-}, HPO_4^{2-}, $H_2PO_4^{1-}$, H_3PO_4, and $CH_3PO_4^{2-}$, respectively, and the single bonds and their shifts are underestimated by 8, −2, 2, and 4%, respectively.

Table 3: The O···P···O angle, P_γ-O Bond Length of GDPO−PO_3^{2-}, P···O Bond Length of the γ-Phosphate Group as a Function of Water−Methyltriphosphate Distance in the Model of the Active Site of ras·MgGTP Complex from ab Initio Calculations in the HF/3-21g* Level

Na·MeTP···H_2 distance (Å)	$\Delta\nu_s(\gamma\text{-}PO_3^{2-})$	$\Delta\nu_a(\gamma\text{-}PO_3^{2-})$	O···P···O angle[a]	P···O bond length (Å)	P_γ−O bond length (Å)
infinite	0	0	114.9	1.513	1.7187
4.0	−3	+2	115.3	1.512	1.7311
3.7	−4	+2	115.3	1.512	1.7331
3.5	−5	+2	115.4	1.512	1.7359
3.25	−6	+1	115.6	1.513	1.7394
3.00	−9	−1	115.8	1.513	1.7447
2.75	−12	−3	116.1	1.513	1.7528
2.50	−18	−8	116.6	1.515	1.7647

[a] Bond angles are in degrees.

α- and β-phosphate groups in aqueous solution, while it binds to only the β-phosphate in ras (*30*).

Similar procedures were performed for the Mg·GTP 1:1 complex (solution model structure **III,** Figure 4) and for the ras·Mg·GTP (structure **IV**). The result of geometry optimization shows that the metal ion binds to the α-, β-, and γ−phosphates in a tridentate manner in the solution model (structure **III**); this is also in agreement with experimental results (*19*). The results are listed in Table 2. To simulate Mg·GTP in the ras complex, a sodium ion was placed between the γ- and β-phosphate groups so that the sodium interacts only with the phosphates as found in the X-ray results. After geometry optimization, the resultant conformation maintains metal ion interaction with the γ- and β-phosphate groups (structure **IV)**, and the results for the γ-PO_3^{2-} group are reported in Table 2. The symmetric and antisymmetric stretch modes of the γ-PO_3^{2-} group are virtually unaffected by the metal ion placed in any geometry that is reasonably close to that found in the X-ray structures compared to the values obtained from the solution model (**III**). Hence, neither mode shows much of a change in frequency in the calculations for various geometries locating the metal ion from structure **III** to **IV**.

However, it is observed experimentally that the symmetric stretch decreases by 10 cm^{-1}, which is a substantial shift. Since, this observed frequency shift of the symmetric stretch mode $\nu_s(\gamma\text{-}PO_3^{2-})$ (Table 1) is not due to the interaction of Mg^{2+} with GTP at the binding site of ras, it is useful to examine alternative interactions. In the crystal structure of GppNp complexed with ras, water-175 is in-line with the phosphorus atom of the γ-phosphate of GTP group at a distance of 3.7 Å (*35*; *36*). To further simulate the Mg·GTP moiety in ras, a water molecule in-line with the bridging P−O bond of methyltriphosphate was placed at various distances, *d* (structure **V**). The geometry of the complex, with the γ-phosphorus−water oxygen distance fixed at various lengths, was optimized with HF/3-21g* basis set. Table 3 shows the results of calculations on several model complexes with P- - -OH_2 distances ranging from 2.5 to 4.0 Å. As can be seen from Table 3, the water molecule can have a rather large effect on the symmetric stretch mode. The reason for this is that the frequencies of the symmetric and antisymmetric stretch modes are functions of bond order (force constant) as well as the angle of the O···P···O bond (see structure **V**, Figure 4). The small interaction between the water molecule and the γ-PO_3^{2-} group does not affect much the bond order of the nonbridging P···O bonds (the P···O bond length is hardly affected; see Table 3). However, the O···P···O bond angle flattens out, i.e., the $-PO_3^{2-}$ constellation becomes more planar, as the water molecule approaches the central phosphorus atom, and this brings about systematic downward shifts in $\nu_s(\gamma\text{-}PO_3^{2-})$ and smaller shifts of $\nu_a(\gamma\text{-}PO_3^{2})$. The best fit to the data is when the water oxygen is about 3.0 Å from the γ-phosphorus; the frequency shift of the symmetric stretch mode $\nu_s(\gamma\text{-}PO_3^{2-})$ (9-cm^{-1}) is close to that observed in the Raman difference spectrum (Table 1). The ab initio results of the stretch frequency shifts are also listed under the heading for the GTP protein complex, structure **V**, Table 2.

Bond Length/Bond Strength/Vibrational Frequency Relationships. For the P···O and P−O bonds of phosphates (and some other metal and nonmetal oxides), there exist very accurate empirically derived relationships between bond length/bond order and bond order/vibrational frequency. Using the definition of bond order or bond strength based on the valence of a given atom (*37*), the sum of the bond orders over all the bonds to the central phosphorus atom is its valence, i.e., 5. The bond orders (bond strengths) are given in terms of valence units in this paper, and labeled as vu, to make it clear that other definitions of bond orders exist (*21*). In this case, the equations are (*20*, *37*, *38*)

$$s_{PO} = (r_{PO}/_{1.620})^{-4.29} \quad (1)$$

where *s* is the bond order of the PO bond (in vu), r_{PO} is the length of the PO bond (in Å), and

$$s_{PO} = [0.175*\ln(224500/\upsilon)]^{-4.29} \quad (2)$$

where υ is the frequency of the phosphate stretch. The symmetric stretch frequency can sometimes be used in s/υ correlations in phosphates (*21*). However, in general, and particularly in situations where the changes in the angle of the O···P···O bonds in the $-PO_3^{2-}$ group are important in affecting the observed shifts of $\nu_s(-PO_3^{2-})$ and $\nu_a(-PO_3^{2-})$ as here, it is necessary to substitute the so-call fundamental stretch frequency into eq 2, which is the geometric average of the symmetric and antisymmetric stretch frequencies, i.e., $\upsilon = [(\nu_s^2 + 2\nu_a^2)/(3)]^{1/2}$ (for dianionic phosphate esters). Hence, bond lengths and bond orders can be determined if the stretch frequencies are known. The error in these relationships is estimated to be about ±0.04 vu and ±0.004 Å for bond orders and bond lengths, respectively, and better at estimating changes in the parameters for a given molecule as it goes from one environment to another (*20*).

Application of these equations for the β-phosphate of Mg·GDP 1:1 complex in aqueous solution, yields $\upsilon = 1066$ cm^{-1} ($\upsilon_s = 942$ cm^{-1} and $\upsilon_a = 1123$ cm^{-1}, Table 1), and a bond order of 1.327 vu and a bond length of 1.517 Å for each of the three nonbridging P···O bonds. For ras-bound Mg·GDP, the fundamental stretch frequency of the P···O bonds of the β-phosphate shifts down to $\upsilon = 1042$ cm^{-1} (Table 1). The shift to lower frequency translates to somewhat lower bond order and longer bond length for each of the three nonbridging terminal P···O bonds: 1.303 vu and 1.523 Å, respectively. This derived bond length for ras-bound Mg·GDP is in excellent agreement with the result from X-ray diffraction studies, 1.528 Å (*30*). Our results show that the total bond order of the nonbridging P···O bonds of the β-PO_3^{2-} group decreases by 0.024 vu when GDP binds to ras. Since the total bond order about the phosphorus atom can be taken to a good approximation to be constant (equal to five), this means that the bridging O−PO_3^{2-} bond increases by 0.072 vu. The β-PO_3^{2-} group of GDP is strongly stabilized when it binds to ras.

For Mg·GTP in aqueous solution, the fundamental frequency of the γ-phosphate is 1065 cm^{-1} from $\upsilon_s = 927$ cm^{-1} and $\upsilon_a = 1128$ cm^{-1} (see Table 1), which yields a bond order of 1.326 vu and a bond length of 1.517 Å for each of the three nonbridging P···O bonds of the γ-phosphate group using eqs 1 and 2. For ras-bound Mg·GTP, the P···O symmetric stretch mode of γ-phosphate shifts down to 917 cm^{-1} (Table 1). The position of υ_a(γ-PO_3^{2-}) for bound GTP has not been definitively assigned. Two bands, at 1128 and 1140 cm^{-1}, are observed in IR studies of rascagedMg·GTP→ras·Mg·GTP (*28*, *29*), and both are good candidates for the antisymmetric stretch (1140 cm^{-1} is favored). It is also possible that the symmetry that gives rise to a degenerate pair of antisymmetric modes has been broken for ras-bound Mg·GTP, in which case the 1128 and 1140 cm^{-1} bands could correspond to two antisymmetric-like modes. In any case, the calculated change upon binding in the bond order (or bond length) of the nonbridging P···O bonds is very small, −0.003 vu or +0.006 vu using 1128 and 1140 cm^{-1} as the extreme ends of the possible position of the antisymmetric stretch, consistent with the ab initio calculations. The downward shift of 10 cm^{-1} for υ_s(γ-PO_3^{2-}) upon binding, and the ab initio analysis above, suggests that the in-line water molecule is interacting with the γ-phosphorus atom of bound GTP. Using eq 1 and a distance of 3.7 Å between in-line water-175 and the γ-phosphorus atom determined from the X-ray study of ras-bound GppNp (*35*, *36*), the bond order[3] of this incipient bond is 0.03 vu.

While the fundamental frequency of a symmetric/antisymmetric set depends chiefly on a force constant, we have shown that the symmetric and antisymmetric modes depend additionally on the angle between the O···P···O bonds (θ in structure **V**, Figure 4) and the ratio of the stretch force constant for the P···O bond to the P···O/P···O stretch/stretch off diagonal force constant, f_s/C_{ss} (*20*). Hence, it is possible to calculate changes in θ once the frequencies and C_{ss} are known. We estimate f_s/C_{ss} for Mg·GTP in aqueous solution by assuming that $\theta = 114.9°$ from the ab initio calculations (Table 3), taking $\upsilon_s = 927$ cm^{-1} and $\upsilon_a = 1128$ cm^{-1}, and applying eqs 7 and 8 of ref *20*. This yields $f_s/C_{ss} = 60/1$. For any angle $\theta > 90°$, a downward shift in υ_s($-PO_3^2$), like the −10 cm^{-1} shift observed when GTP binds to ras, implies an increase of θ (see eqs 7 and 8, ref *20*). The amount of increase is affected by the value of antisymmetric mode, which is uncertain. Considering the range in the possible values for υ_a, $\Delta\theta = +1.1°$ for $\upsilon_s = 917$ cm^{-1} and $\upsilon_a = 1128$ cm^{-1} or $\Delta\theta = +2.3°$ for $\upsilon_s = 917$ cm^{-1} and $\upsilon_a = 1140$ cm^{-1}. This is in fair agreement with the ab initio calculations which yield a $\Delta\theta = +0.9°$ (compare the 3.00 Å row with the infinite row of Table 3). This angle change is relatively small, and this is consistent with the weak interaction that water-175 has with bound GTP in ras. As a comparison, it is observed that the widths of antisymmetric stretch modes of dianionic monoesters in solution are quite broad (32 cm^{-1} fwhm for GTP; ref *19*) while those of symmetric stretch modes are relatively narrow (less than 10 cm^{-1} for GTP). The reason for this is that θ adopts a range of angles by thermal motion, and this shows up as a range in the value of f_s as well. The two changes cancel for the symmetric stretch but are additive for the antisymmetric stretch according to eqs 7 and 8 of ref *20* when $\theta > 90$. Hence, the width of the antisymmetric mode arises from heterogeneous broadening. From the width of the antisymmetric stretch, we estimate that the angle of O···P···O of the $-PO_3^{2-}$ moiety undergoes an excursion of about 2.7° (±0.5°) for GTP in aqueous solution due to thermal motion.

DISCUSSION

Vibrational frequencies are determined by the force constants within chemical bonds and the geometry of the atoms that make up a molecule. Hence, vibrational frequencies report on bond orders, bond lengths, and geometry. A clear result from our investigation is that the ionization state of GDP or GTP does not change from its solution value when these nucleotides bind to the ras protein. This is so because the frequencies associated with the stretch motions of the various P···O bonds of bound GDP and GTP are not altered to the extent that would indicate protonation of one or more of these bonds. Such a protonation of the γ-PO_3^{2-} moiety of bound GTP would be found if substrate-assisted catalysis occurred such that bound GTP activates an attacking water molecule by abstracting a proton to form hydroxyl. This has been postulated to occur (*13*, *39*, *40*). Our results rule out a significant population of protonated bound GTP, but do not rule out a minor population or one that is formed transiently.

Divalent cations are generally located in the binding sites of nucleotide phosphotransferases and complex directly to oxygens of bound phosphates, thereby strongly affecting binding of GDP and GTP as well as GTPase activity (*1*, *41*, *42*). For ras, Mg^{2+} forms a very tight complex with GDP which reduces, for example, the GDP dissociation rate by 4 orders of magnitude compared to Mg^{2+}-free ras (*42*). On the other hand, the dissociation rate of GTP is enhanced by only about a factor of 10 in Mg^{2+}-free ras (*43*).

On the basis of the present studies of the ras·Mg·GDP and ras·Mg·GTP complexes, the following structural conclu-

[3] This must be considered approximate. The empirical relationship given by eq 1, which holds over a broad range of bond orders, has not, however, been tested for such low bond orders. In addition, the distance between water-175 and the γ-phosphorus atom of bound GppNp may not be the same as for bound GTP.

sions can be made. In the first place, it seems likely that the binding site Mg^{2+} ion is substantially responsible for the observed frequency shifts of ras-bound GDP, and so a dominating factor in how the β-phosphate moiety of GDP interacts with the ras binding site. This is so for the following reasons. Although the X-ray structure of ras·Mg·GDP shows that a number of hydrogen bonds are formed between binding site residues of ras and the β-PO_3^{2-} group of GDP, these are noncharged polar groups. Such groups generally make much smaller contributions to electrostatic interactions than groups that carry charge. In addition, the ab initio calculations show that the interaction between Mg^{2+} and GDP at the binding site can easily account for the observed frequency changes at the β-phosphate. Thus, the frequency shifts of the specific P···O bonds of bound GDP indicate that Mg^{2+} interacts with ras-bound GDP only with the β-phosphate group, in agreement with a previous EPR study (*44*). This is in contrast to Mg·GDP complexes in solution, where vibrational studies indicate that there is a bidentate interaction of Mg^{2+} to the α- and β-phosphates (*19*). Hence, the frequencies of β-PO_3^{2-} for ras-bound GDP are decreased upon binding relative to Mg·GDP in solution while those of the α-PO_2^- group increase. This coordination pattern is in agreement with the X-ray studies of ras·Mg·GDP (*30*, *35*). Nevertheless, the relative importance of the active site polar groups in affecting the electronic properties of bound nucleotides requires a systematic study, perhaps through the use of mutant proteins in vibrational studies and through modeling.

The nonbridging P···O bonds of the β-PO_3^{2-} group of bound GDP are strongly polarized upon binding to ras, reducing their bond order by 0.024 vu from the Mg·GDP solution value (equal to 1.327 vu) and increasing the average P···O bond length by 0.006 Å. This indicates a strong favorable electrostatic interaction between the binding site Mg^{2+} and GDP. The Brown and Wu paradigm (*37*) states that the sum of all bonds about a phosphorus atom be equal to 5 (the valence of phosphorus), so that the weakening of the nonbridging P···O bonds of the β-PO_3^{2-} group results in a strengthening of the bridging GMPO−PO_3^{2-} bond of 0.072 vu. It is clear that the terminal β-phosphate group of bound GDP interacts strongly with the ras binding site and that GDP is energetically stabilized. For bound GTP, the binding site Mg^{2+} maintains its interaction with the β-phosphate group as judged by the shifts in the υ_a(β-PO_2^-) band from its solution value (refs *28*, *29*; Table 1). Hence, the bonds of the β-phosphate of both bound GDP and GTP are strongly polarized, indicating a substantial interaction with the ras binding site. In contrast, the P···O bonds of the γ-PO_3^{2-} group of GTP are little affected by binding to ras since there is only a very small change in their bond polarization as calculated in Results.

As shown by the modeling results and the analytical relationships relating these stretch frequencies to force constant and angle (see Results), the small 10 cm^{-1} downward shift of the symmetric stretch mode of bound GTP, υ_s(γ-PO_3^{2-}), is well explained by about a 1−2° increase in the O···P···O angle (θ in structure **V**, Figure 4), approaching the $\theta = 120°$ for a planar PO_3 moiety, with little change in bond order. Hence, the structure of the γ-PO_3^{2-} group of ras-bound GTP is such that the three nonbridging P···O bonds approach a more planar arrangement compared to GTP in solution. The ab initio calculations suggest that the binding site Mg^{2+} is unable to produce even this small frequency shift for υ_s(γ-PO_3^2). Its geometry relative to the terminal phosphate group is such that its effect through electrostatic interactions is calculated to produce negligible changes in the symmetric and antisymmetric stretch modes of the γ-PO_3^{2-} group. On the other hand, a water molecule in-line to the γ-phosphate, structure **V** of Figure 4, can reproduce the experimentally observed shift because of their relative geometry. The ab initio calculations place the water molecule at a P−OH_2 distance of 3.0 Å to yield the correct shift in υ_s(γ-PO_3^{2-}) (Table 3). This can be considered to be in good agreement with the 3.7-Å distance observed for water-175 in the ras·GppNp crystal structure, considering that our results are on the ras·GTP complex while the X-ray determined distance is of the ras·GppNp complex and also considering the inaccuracies in the calculations.

Generally, theories of phosphotransfer reactions for dianionic phosphate monoesters have a pentacoordinated phosphorus transition state in which the nonbridging P···O bonds become planar and the leaving group and attacking nucleophile form apical bonds. Such a transition state is consistent for ras on the basis of crystal structures of guanine-binding proteins with bound GDP·ALF_4^- (*1*), which is believed to resemble the transition state of the pathway, and by studies of the hydrolysis stereochemistry in ras, which suggest a direct in-line transfer of the γ-phosphate from GTP to water with inversion of the configuration (*45*). With this in mind, the 1−2° angle increase of the nonbridging O···P···O bonds toward a planar geometry of the γ-phosphate can be considered. It is clear that the ground state of GTP is destabilized by its binding to ras in such a way that a small but a clear geometry change takes place that brings bound GTP closer to its transition state geometry. There has been much discussion of the role of Gln-61 in GTP hydrolysis since mutations of this residue reduce the hydrolysis rate 10-fold or so and it is within hydrogen bonding distance to water-175, which is generally believed to be the attacking nucleophile. Several possible catalytic roles have been advanced for this residue. One theory has this residue activating water-175 by abstracting a proton to form the stronger hydroxyl nucleophile for attack (*35*, *46*). This might occur even though the amide of Gln-61 is a weak base in water when the entire binding site structure is considered (*39*). Another possibility that has been advanced is that the functional group of Gln-61 participates in a proton shuttle that finally protonates the γ-phosphate of bound GTP (*47*). Finally, it has been supposed that it could help stabilize the formation of negative charge on the attacking water nucleophile or negative charge on the phosphate oxygens in the transition state (*40*, *48*). Our results suggest, rather, that it may have an important structural role in that it, and other residues interacting with water-175, hold this water close enough and tight enough to the phosphorus atom of the γ-phosphate to cause a significant interaction between them. The calculations from the empirical relationships relating bond distance and bond order indicate a small incipient fifth bond between water-175 and the γ-phosphorus atom of GTP of approximately 0.03 vu. In addition to bringing the geometry of the bound GTP closer to its transition state, this interaction weakens the bridging GDPO−PO_3^{2-} bond in the ground state by a corresponding amount since most of the

bond order formed by the phosphorus atom with water-175 is taken from the bridging bond (see Results).

This study does not directly speak to the electronic nature of the transition state structure, that is whether it is dissociative (one where the sum of the apical bonds is close to zero) or associative (wherein there is considerable bond formation between the attacking nucleophile before much bond breaking with the leaving group) or concerted (S_n2-like), because our results are on ground state complexes. However, the results are highly suggestive of a concerted transition state where the bond formation is more or less synchronous with the bond cleavage of the GDP leaving group based on the following reasoning. In the ground state, there is a small formation of the incipient fifth bond between water-175 and corresponding weakening of the O−P bond between the GDP leaving group and the γ-phosphorus of bound GTP. This state presumably shows some transition state character and so suggests a concerted mechanism. In addition as discussed above, the active site Mg^{2+} ion (with perhaps other active site residues) interacts more strongly with the P···O bonds of the GDP leaving group β-phosphate than with the γ-phosphate of bound GTP. This interaction would appear to impose stabilization of the GDP leaving group while the γ-phosphate forms the bond with the attacking (water) nucleophile, prior to release of inorganic phosphate. Finally, results on a Mg^{2+}·ADP·vanadate complex bound to myosin subfragment 1, which is believed to resemble the transition state of the ATPase reaction catalyzed by myosin, show that the sum of the bond orders of the two apical bonds involving the attacking water molecule and the ADP leaving group is little changed upon binding, as expected for a concerted reaction (*49*). Hence, assuming the reaction pathway of the ras and S1 enzymes are similar, this result reinforces the notion that the process in both proteins has concerted mechanisms.

ACKNOWLEDGMENT

We thank Drs. V. Cepus, C. Ulbrich, C. Allin, A. Troullier, and K. Gerwert for showing us their manuscript prior to publication.

APPENDIX

We show in this section the procedure used to obtain the difference spectra presented in the main article. In general, Raman difference spectroscopy requires a high degree of precision in calculating the difference spectrum, and it is necessary that the instrument be calibrated to ensure that neither systematic noise factors nor shot noise are mistaken for small difference peaks (*16*). We show here the control procedures that were performed in determining the data of Figure 2b. All the other difference spectra presented herein underwent the same procedures.

The ras·Mg·GTP and ras·Mg·(β-$^{18}O_2$;$\beta\gamma$-^{18}O)GTP complexes were loaded into the separate compartments of a split Raman cell, and Raman spectra were taken alternatively from the two samples. Typically about 10 runs were taken from each sample, and they were then summed and averaged. The averaged spectrum so obtained for the ras·Mg·GTP complex is shown in Figure 5a while Figure 5b shows that of ras·Mg·(β-$^{18}O_2$;$\beta\gamma$-^{18}O)GTP. As a control experiment, the odd-numbered runs and even-numbered runs on the ras·Mg·GTP sample were averaged, and their difference spectrum is shown in Figure 5c (enhanced by a factor of 20 relative to Figure 5a). This difference spectrum, which would null completely in an ideal case, is a strong indicator of ultimate noise levels. The noise in this spectrum, all of which is simple shot noise and is free from systematic subtraction artifacts, is 0.2% of the strongest protein band at 1003 cm^{-1} which is adequate for the present studies.

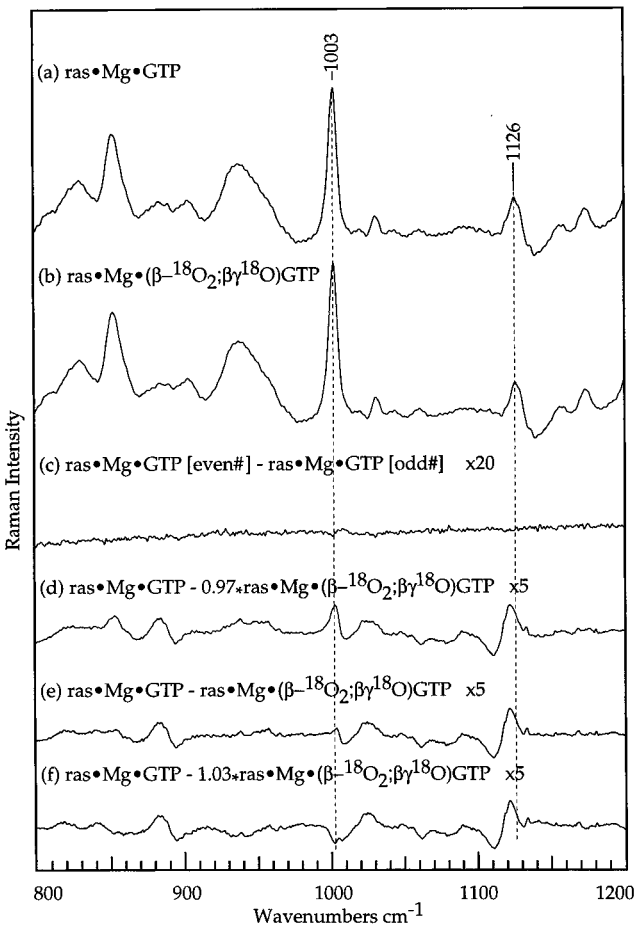

FIGURE 5: (a) Raman spectrum of ras·Mg·GTP, (b) Raman spectrum of ras·Mg·(β-$^{18}O_2$;$\beta\gamma$-^{18}O)GTP, (c) difference spectrum of even-numbered ras·Mg·GTP runs minus odd-numbered runs, the result was then multiplied by a factor of 20, (d) difference spectrum between ras·Mg·GTP and ras·Mg·(β-$^{18}O_2$;$\beta\gamma$-^{18}O)GTP, a factor of 0.97 was multiplied on the latter spectrum and the result multiplied by a factor of 5, (e) difference Raman spectrum between ras·Mg·GTP and ras·Mg·(β-$^{18}O_2$;$\beta\gamma$-^{18}O)GTP, same as Figure 2b, (f) difference spectrum between ras·Mg·GTP and ras·Mg·(β-$^{18}O_2$;$\beta\gamma$-^{18}O)GTP, a factor of 1.03 was multiplied on the latter spectrum and the result multiplied by a factor of 5.

In the subtraction process, several protein Raman bands were used as internal references, and the bands at 1003 and 1126 cm^{-1} are indicated in the Figure. A multiplication factor was applied to one of the spectra, and adjusted, so that in the final difference spectrum these two bands were no longer visible. Since the peak-to-peak intensity in the spectrum of the control (Figure 5c) is about 0.2% of the 1003 cm^{-1} band intensity of the original spectrum, we expect that the noise level in the ras·Mg·GTP minus ras·Mg·(β-$^{18}O_2$;$\beta\gamma$-^{18}O)GTP difference spectrum to be the same. Figure 5e shows the ras·Mg·GTP minus ras·Mg·(β-$^{18}O_2$;$\beta\gamma$-^{18}O)GTP difference spectrum, with both 1003 and 1126 cm^{-1} bands subtracted properly. Of Figure 5, parts d and f, show the

slightly under-subtracted and over-subtracted difference spectra, respectively. In these two spectra, both the 1003 and 1126 cm^{-1} bands are clearly visible, either positive or negative. The intensities of the spectra in Figure 5, parts d and f were enhanced by a factor of 5 relative to the scale of Figure 5a for clarity. The intensities of the difference peaks in Figure 5e are about 2−3% of the intensity of the original spectrum's 1003 cm^{-1} peak. Hence, the signal-to-noise in the difference spectrum is about or greater than 10/1.

REFERENCES

1. Sprang, S. R. (1997) *Annu. Rev. Biochem. 66*, 639−678.
2. Kjeldgaard, M., Nyborg, J., and Clark, B. F. C. (1996) *FASEB J. 10*, 1347−1368.
3. Bourne, H. R., Sanders, D. A., and McCormick, F. (1990) *Nature 348*, 125−131.
4. Bourne, H. R., Sanders, D. A., and McCormick, F. (1991) *Nature 349*, 117−127.
5. Herschlag, D., & Jencks, W. P. (1990) *Biochemistry 29*, 5172−5179.
6. Zhang, M., Zhou, M., Van Etten, R. L., and Stauffacher, C. (1997) *Biochemistry 36*, 15−23.
7. Deng, H., Ray, W. J., Burgner, J. W., and Callender, R. (1993) *Biochemistry 32*, 12984−12992.
8. Weiss, P. M., and Cleland, W. W. (1989) *J. Am. Chem. Soc. 111*, 1928−1929.
9. Jones, J. P., Weiss, P. M., and Cleland, W. W. (1991) *Biochemistry 30*, 3634−3639.
10. Hengge, A. C., Sowa, G. A., Wu, L., and Zhang, Z.-Y. (1995) *Biochemistry 34*, 13982−13987.
11. Hengge, A. C., Denu, J. M., and Dixon, J. E. (1996) *Biochemistry 35*, 7084−7092.
12. Hengge, A. C., Zhao, Y., Wu, L., and Zhang, Z.-Y. (1997) *Biochemistry 36*, 7928−7936.
13. Schweins, T., and Warshel, A. (1996) *Biochemistry 35*, 14232−14243.
14. Hollfelder, F., and Herschlag, D. (1995) *Biochemistry 34*, 12255−12264.
15. Zhao, Y., and Zhang, Z.-Y. (1996) *Biochemistry 35*, 11797−11804.
16. Callender, R., and Deng, H. (1994) *Annu. Rev. Biophys. Biomol. Struct. 23*, 215−245.
17. Weng, G., Manor, D., Chen, Z., Balogh-Nair, V., and Callender, R. (1994) *Protein Sci. 3*, 22−29.
18. Manor, D., Weng, G., Deng, H., Cosloy, S., Chen, C. X., Balogh-Nair, V., Delaria, K., Jurnak, F., and Callender, R. H. (1991) *Biochemistry 30*, 10914−10920.
19. Wang, J. H., Xiao, D. G., Deng, H., Callender, R., and Webb, M. (1998) *Biospectrscopy* (in press).
20. Deng, H., Wang, J. H., Callender, R., and Ray, W. J. J. (1998) *J. Phys. Chem. B 102*, 3617−3623.
21. Ray, J. W. J., Burgner, I. J. W., Deng, H., and Callender, R. (1993) *Biochemistry 32*, 12977−12983.
22. Tucker, J., Sczakiel, G., Feurstein, J., John, J., Goody, R. S., and Wittinghofer, A. (1986) *EMBO J. 5*, 1351−1358.
23. John, J., Sohmen, R., Feurstein, J., Linke, R., Wittinghofer, A., and Goody, R. S. (1990) *Biochemistry 29*, 6058−6065.
24. Darwish, A. A., and Prichard, R. K. (1981) *J. Liq. Chromatogr. 4*, 1511−1524.
25. Miller, D. L., and Weissbach, H. (1974) *Adv. Enzymol. 30*, 219−232.
26. Deng, H., Zheng, J., Burgner, J., Sloan, D., and Callender, R. (1989) *Biochemistry 28*, 1525−1533.
27. Yue, K. T., Deng, H., and Callender, R. (1989) *J. Raman Spectrosc. 20*, 541−546.
28. Cepus, V., Ulbrich, C., Allin, C., Troullier, A., and Gerwert, K. (1998) in *Methods Enzymol.* (in press).
29. Cepus, V., Goody, R. S., and Gerwert, K. (1988) *Biochemistry* (submitted).
30. Tong, L., de Vos, A. M., Milburn, M. V., and Kim, S. H. (1991) *J. Mol. Biol. 217*, 503−516.
31. Deng, H., Zheng, J., Sloan, D., Burgner, J., and Callender, R. (1992) *Biochemistry 31*, 5085−5092.
32. Deng, H., Huang, L., Groesbeek, M., Lugtenburg, J., and Callender, R. H. (1994) *J. Am. Chem. Soc. 98*, 4776−4779.
33. Huang, L., Deng, H., Koutalos, Y., Ebrey, T., Groesbeek, M., Lugtenburg, J., Tsuda, M., and Callender, R. H. (1996) *Biochemistry 35*, 8504−8510.
34. Tsuboi, M., Nishimura, Y., Hirakawa, A. Y., and Peticolas, W. L. (1987) in *Biological Application of Raman Spectroscopy* (Spiro, T. G., Ed.) John Wiley & Sons, New York.
35. Pai, E. F., Krengel, U., Petsko, G. A., Goody, R. S., Kabsch, W., and Wittinghofer, A. (1990) *EMBO J. 9*, 2351−2359.
36. Wittinghofer, A., Krengel, U., John, J., Kabsch, W., and Pai, E. F. (1991) *Environ. Health Perspect.* 11−15.
37. Brown, I. D., and Wu, K. K. (1976) *Acta Crystallogr. B32*, 1957−1959.
38. Hardcastle, F. D., and Wachs, I. E. (1991) *J. Phys. Chem. 95*, 5031−5041.
39. Langen, R., Schweins, T., and Warshel, A. (1992) *Biochemistry 31*, 8691−8696.
40. Schweins, T., Geyer, M., Scheffzek, K., Warshel, A., Kalbitzer, H. R., and Wittinghofer, A. (1995) *Nat. Struct. Biol. 2*, 36−44.
41. Gilman, A. G. (1987) *Annu. Rev. Biochem. 56*, 615−649.
42. John, J., Rensland, H., Schlichting, I., Vetter, I., Borasio, G. D., Goody, R. S., and Wittinghofer, A. (1993) *J. Biol. Chem. 268*, 923−929.
43. John, J., Frech, M., and Wittinghofer, A. (1988) *J. Biol. Chem. 263*, 11792−11799.
44. Feuerstein, J., Kalbitzer, H. R., John, J., Goody, R. S., and Wittinghofer, A. (1987) *Eur. J. Biochem. 162*, 49−55.
45. Feuerstein, J., Goody, R. S., and Webb, M. R. (1989) *J. Biol. Chem. 264*, 6188−6190.
46. Frech, M., Darden, T. A., Pedersen, L. G., Foley, C. K., Charifson, P. S., Anderson, M. W., and Wittinghofer, A. (1994) *Biochemistry 33*, 3237−3244.
47. Sondek, J., Lambright, D. G., Noel, J. P., Hamm, H. E., and Sigler, P. B. (1994) *Nature 372*, 276−279.
48. Prive, G. G., Milburn, M. V., Tong, L., De Vos, A. M., Yamaizumi, Z., Nishimura, S., and Kim, S. H. (1992) *Proc. Natl. Acad. Sci. U.S.A. 89*, 3649−3653.
49. Deng, H., Wang, J., Callender, R. H., Grammer, J. C., and Yount, R. G. (1998) Biochemistry (in press).

BI980471M